

# Optimization at the Interface of Unitary and Non-unitary Quantum Operations in PCOAST

Albert T. Schmitz<sup>\*‡</sup>, Mohannad Ibrahim<sup>\*</sup>, Nicolas P. D. Sawaya<sup>†</sup>, Gian Giacomo Guerreschi<sup>†</sup>, Jennifer Paykin<sup>\*</sup>, Xin-Chuan Wu<sup>†</sup>, and A. Y. Matsuura<sup>\*</sup>

<sup>\*</sup> Intel Labs, Intel Corporation, Hillsboro, OR, USA

<sup>†</sup> Intel Labs, Intel Corporation, Santa Clara, CA, USA

<sup>‡</sup> Email: albert.schmitz@intel.com

**Abstract**—The Pauli-based Circuit Optimization, Analysis and Synthesis Toolchain (PCOAST) was recently introduced as a framework for optimizing quantum circuits. It converts a quantum circuit to a Pauli-based graph representation and provides a set of optimization subroutines to manipulate that internal representation as well as methods for re-synthesizing back to a quantum circuit. In this paper, we focus on the set of subroutines which look to optimize the PCOAST graph in cases involving unitary and non-unitary operations as represented by nodes in the graph. This includes reduction of node cost and node number in the presence of preparation nodes, reduction of cost for Clifford operations in the presence of preparations, and measurement cost reduction using Clifford operations and the classical remapping of measurement outcomes. These routines can also be combined to amplify their effectiveness.

We evaluate the PCOAST optimization subroutines using the Intel<sup>®</sup> Quantum SDK on examples of the Variational Quantum Eigensolver (VQE) algorithm. This includes synthesizing a circuit for the simultaneous measurement of a mutually commuting set of Pauli operators. We find for such measurement circuits the overall average ratio of the maximum theoretical number of two-qubit gates to the actual number of two-qubit gates used by our method to be 7.91.

**Index Terms**—quantum computing, quantum circuit optimization, Pauli optimization

## I. INTRODUCTION

PCOAST, a Pauli-based Circuit Optimization, Analysis, and Synthesis Toolchain, was recently introduced as a comprehensive framework for quantum circuit optimization [1]. It draws on a class of unitary quantum circuit optimizations based on Pauli rotations [2, 3, 4] that take advantage of the fact that unitary circuits can be decomposed into Clifford gates and Pauli rotations  $\text{Rot}(P, \theta) = e^{-i\theta/2P}$ , where  $P$  is a Pauli matrix  $X$ ,  $Y$ , or  $Z$ . Because Cliffords always map Paulis to Paulis by conjugation, it is possible to push Clifford unitaries  $U$  past the non-Clifford Pauli rotations  $\text{Rot}(P, \theta)$  to produce a new rotation  $\text{Rot}(UPU^\dagger, \theta)$ . Doing so can expose the fact that some rotations can be merged [2].

PCOAST extends these optimizations into a comprehensive framework in several key ways. First, it introduces the PCOAST graph whose nodes represent quantum operations with edges based on the non-commutativity of the underlying Pauli operators. While prior work was limited to unitary optimizations, PCOAST acts on mixed unitary and non-unitary circuits by introducing preparation and measurement nodes parameterized by Paulis alongside unitary rotations and Clifford

nodes. Second, PCOAST introduces a customizable greedy synthesis algorithm to synthesize efficient gate representations from the PCOAST graph. And finally, PCOAST implements sophisticated internal optimizations on the PCOAST graph, which are the focus of this paper.

This paper presents the details of those PCOAST-to-PCOAST graph optimizations primarily aimed at exploiting the interaction between unitary and non-unitary nodes. These optimizations include reducing both the cost and number of non-Clifford nodes in the presence of preparations and the cost of Clifford operations in the presence of preparations. However, the most impactful of these optimizations is the reduction of mutually commuting measurements and their cost using Clifford operations and classical measurement remapping. Though other methods exist [5, 6, 7], we demonstrate that our methods:

- make no additional restriction on the measurement set;
- leverage full and partial qubit agreement (see Defn. 4);
- have no limit on size or independence of the Pauli measurement set;
- leverage lower-weight elements in the span of the measurement set to minimize the circuit costs; and
- are fully integrated into the PCOAST framework, and inherit its efficiencies, refinements, and scalability[1] including future development.

All methods discussed throughout the paper are implemented in the Intel<sup>®</sup> Quantum Software Development Kit (SDK)<sup>1</sup> [8], including the automated remapping of measurement results.

The structure of the paper is as follows: In Section II, we motivate the set of optimization implemented by PCOAST, before giving some theoretical background in Section III. We then discuss the Stabilizer Search Problem and our solution to it in Section IV as well as the optimization of unitary channels in the presence of preparations in Section V. Section VI combines these into a full optimization scheme. In Section VII, we evaluate the performance of our methods for the Variational Quantum Eigensolver (VQE) algorithm where we find an overall average ratio of the maximum theoretical number of two-qubit gates to the actual number of two-qubit gates used by our method to be 7.91. This is compared to the value of 3.5 as found for a similar metric using the best known existing

<sup>1</sup><https://developer.intel.com/quantumSDK>

solution to the Stabilizer Search problem[7]. Finally, we make concluding remarks in Section VIII.

## II. MOTIVATION

Much of PCOAST’s efficacy comes from the structure of the PCOAST graph, primarily by exploiting commutativity of the operations. This allows for merging of some operations and synthesizing of a more optimal ordering when implemented. However, this alone is not enough to capture many known simplifications, especially at the interfaces of unitary and non-unitary elements. Fig. 1 shows some common quantum circuit optimizations involving preparations. Each of these is an example of a unitary controlled on a qubit prepared in a computational state and is not captured by the structure of the PCOAST graph on its own. Furthermore, the result of each example translates to the PCOAST graph differently, and optimizations which capture and generalize these have to be handled separately. This is not a drawback, however, because the generalization can express otherwise non-intuitive relations that go well beyond simple pattern matching. We demonstrate this process in Section V.

Another opportunity for optimization using PCOAST comes from a mutually commuting set of measurement nodes occurring at the end of a PCOAST graph. Such a case occurs when the graph is built from a quantum circuit that ends by measuring most or all of its qubits. A similar situation occurs when measuring an arbitrary Hamiltonian for the broad class of VQE algorithms [9, 10, 11] or any other class which requires the expectation value of a Hermitian observable. Though other methods exist [12, 13, 14], a common strategy for extracting expectation values is to expand the operator in the Pauli operator basis, then group the terms of that expansion into mutually commuting sets. These sets can either be qubit-wise commuting [5], fully commuting [6] or sorted for the sake of minimizing total shots on the quantum computer [7]. The qubit-wise commutation case has a direct translation to a circuit—a single-qubit basis change to the agreed single-qubit Pauli operator support (see Defn. 4). In the latter two cases, however, the authors generate a Clifford circuit to extract a set of simultaneous measurements capable of reconstructing all elements. (see Defn. 3 for a formal description).

When applying synthesis to a PCOAST graph with mutually commuting Pauli measurements at the end, the greedy synthesis algorithm described in Ref. [1] can generate seemingly odd behavior, as shown in Fig. 2. Here, we see that several measurements are performed on the same qubit, and CNOT gates are used to perform a binary sum over classical variables which could be performed by classical resources. Moreover, gate action after the measurements may cause problems if the measurements on the underlying qubit system are destructive. This behavior cannot be remedied by simply replacing the sequence of measurement and Clifford gates with some equivalent sequence as described by the Refs. [5, 6, 7], as there is an implicit promise that the resulting quantum channel action is fully equivalent to what was originally specified, including the end quantum state returned by the channel. We

refer to this as the *end-state promise*. The end-state promise even applies when the qubit states are fully measured and entanglement is completely removed. Baring some classical feedback mechanism, synthesis does not know a priori what the outcomes will be and has no choice but to use Clifford gates to reconstruct the classical state and meet the promise. However, there are many situations where the end-state is irrelevant. This leaves two possible desired outcomes:

- 1) A *hold outcome* indicates that the quantum state is in part or in whole a desired return of the program. Thus we must meet the end-state promise.
- 2) A *release outcome* indicates that the desired results are the measurement outcomes only. Once all measurement results have been recorded, the quantum state can be “released” and we make no promises on the final state of the quantum system. More formally:

**Definition 1.** A release outcome is represented by an equivalence class defined by a set of measurables,  $M = \{m_i\}$ , of quantum channels such that  $C$  is equivalent to  $C'$  relative to  $M$  if and only if  $\text{Tr}(C(\rho)m_i) = \text{Tr}(C'(\rho)m_i)$  for each  $i$  and for all states  $\rho$ .<sup>2</sup>

In the case of a PCOAST graph,  $M$  is represented by the measurement nodes of the graph, which is implied when discussing a release outcome.

For most algorithms or quantum submodules, a release outcome is sufficient, including variational algorithms such as VQE, Thermofield double state preparation [15, 16], and imaginary-time evolution [17, 18], to name a few. Hold outcomes are typically only required for submodules where partial measurements are used to update the state in real-time, such as syndrome extraction for error correction or repeat-until-success routines [19, 20].

In the case of a release outcome, we are free to replace a set of mutually commuting measurements with an equivalent, more efficient set of measurements. In Section IV, we propose a method for simultaneously deriving both an equivalent set of measurements as well as a circuit realizing them.

## III. BACKGROUND

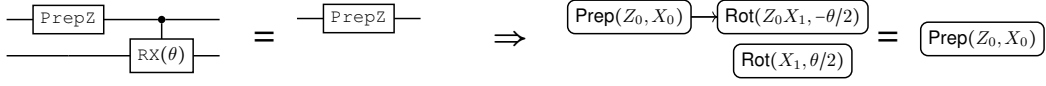
### A. The Pauli group

A single-qubit Pauli is one of  $X, Y, Z$ , defined as the  $2 \times 2$  matrices,

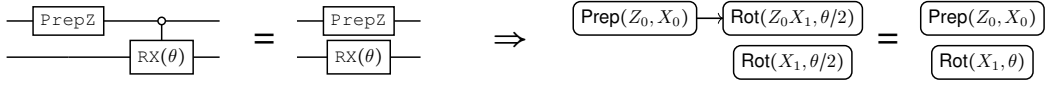
$$X = \begin{pmatrix} 0 & 1 \\ 1 & 0 \end{pmatrix} \quad Y = \begin{pmatrix} 0 & -i \\ i & 0 \end{pmatrix} \quad Z = \begin{pmatrix} 1 & 0 \\ 0 & -1 \end{pmatrix}, \quad (1)$$

or the identity  $I$ . At times we use  $\sigma \in \{X, Y, Z\}$  to represent an arbitrary, non-identity single-qubit Pauli. A Pauli operator,  $P$ , on  $N$  qubits is then the tensor product of any combination of single-qubit Paulis, scaled by a constant phase( $P$ )  $\in \{1, -1, i, -i\} \simeq \mathbb{Z}_4$ . By convention, the canonically positive version of a Pauli operator is the one which can

<sup>2</sup>This definition is equivalent to that provided in [1], as written in terms of *classical-quantum states*, where  $M$  corresponds the space of measurement outcomes described therein.



(a) Positive control on a qubit prepared in the  $|0\rangle$  state is equivalent to just the preparation.



(b) Negative control on a qubit prepared in the  $|0\rangle$  state is equivalent to just the preparation and the uncontrolled unitary.



(c) Equivalent example as Fig. 1a but in this case, the unitary is a Clifford, represented by a Pauli frame (see Sec III-C).



(d) Similar to Fig. 1c but here we demonstrate the resulting PCOAST interpretation on downstream measurements for a release outcome.

Fig. 1: Simple optimizations following preparations, and the corresponding optimizations on PCOAST graphs.

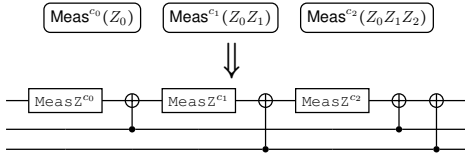


Fig. 2: Example of how PCOAST circuit synthesis may handle measurements because it must meet an end-state guarantee implied by the PCOAST graph representation.

be written as such with the phase  $1 \in \mathbb{Z}_4$ . This collection of operators can be understood as the *Pauli group*,  $\mathcal{G}_N$ , under matrix multiplication. The support of an  $N$ -qubit Pauli operator,  $\text{supp}(P)$ , is the set of indices  $i$  for which  $(P)_i \neq I$ . We write  $X_i$ ,  $Y_i$ , and  $Z_i$  for Paulis with support  $\{i\}$ .

An important feature of the Pauli group is that any two members  $P_1, P_2 \in \mathcal{G}_N$  either commute or anti-commute. We capture this in the function  $\lambda: \mathcal{G}_N \times \mathcal{G}_N \rightarrow \mathbb{F}_2$ ,

$$\lambda(P_1, P_2) = \begin{cases} 0 & P_1 \text{ commutes with } P_2 \\ 1 & \text{otherwise} \end{cases} \quad (2)$$

We have, therefore, that  $P_1 \cdot P_2 = (-1)^{\lambda(P_1, P_2)} P_2 \cdot P_1$ .

### B. The Pauli Space

Throughout this paper, the phase factor of the Pauli group,  $\mathbb{Z}_4$ , tends to function as a hindrance to the understand of our optimizations and their functioning. This is the case because of the overwhelming use of the Hermitian versions of Pauli operators (i.e. when  $\mathbb{Z}_4$  is restricted to  $\{1, -1\} \simeq \mathbb{Z}_2$ ) and the ability for the distinction between the canonically positive and negative version of a Pauli operator to be absorbed by other mechanisms. As such, we define the *Pauli space* as  $\mathcal{P}_N = \mathcal{G}_N / \mathbb{Z}_4$ . The Pauli space abelianizes the Pauli

TABLE I: Overview of the correspondence between the Pauli Group and the Pauli Space. The use and interpretation of this notation should be clear in the context in which it is used.

Notion	Pauli Group	Pauli Space
membership	$P \in \mathcal{G}_N$	$p = [P] \in \mathcal{P}_N$
scalar action ( $a \in \mathbb{F}_2$ )	$P^a$	$ap$
group action	$P * Q$	$p + q$
identity	$I$	$0$
2-form	$\lambda(P, Q)$	$\lambda(p, q)$
Clifford action	$\vec{F}(P) = UPU^\dagger$	$f(p)$

group, and thus can be understood as a binary vector space  $\mathcal{P}_N \simeq \mathbb{Z}_2^{\otimes 2N}$  [21]. From this perspective, multiplication is lifted to binary addition, implying  $I$  is the additive identity, multiplicative power is lifted to scalar multiplication and the binary field  $\mathbb{F}_2$  is appropriate since  $P^2 \propto I$  in  $\mathcal{G}_N$ . An overview of this mapping is show in Table I. We denote the lift of a Pauli operator  $P \in \mathcal{G}_N$  to its  $p \in \mathcal{P}_N$  equivalence class via square brackets,  $p = [P]$ , and implicitly always map members of  $\mathcal{P}_N$  to their canonically positive element in  $\mathcal{G}_N$ . Although we lose the commutation relations, we can reintroduce them by extending  $\mathcal{P}_N$  to a *symplectic* vector space, by treating  $\lambda$  as a symplectic form (as restricted to  $\mathcal{P}_N$ ).<sup>3</sup>

### C. Pauli Frame as Pauli Space Automorphism

Pauli tableaus [22] were first introduced as a way to simulate stabilizer states generated entirely from Clifford gates ( $H$ ,  $S$ , and  $CNOT$ ) and single-qubit measurements. Since then, Pauli tableaus have been used to represent Clifford circuits in general, not just for the purposes of stabilizer simulation.

<sup>3</sup>The necessary feature of a symplectic form  $\lambda$  are for  $p, q, r \in \mathcal{P}_N$ :  $\lambda(p + q, r) = \lambda(p, r) + \lambda(q, r)$ ,  $\lambda(p, p) = 0$ , and  $p = 0$  if and only if  $\lambda(p, q) = 0$  for all  $q \in \mathcal{P}_N$ . Note that these conditions imply  $\lambda(p, q) = \lambda(q, p)$  in the binary case. Also for a subset  $\mathcal{G} \subseteq \mathcal{P}_N$ , we define  $\mathcal{G}^\perp = \{p \in \mathcal{P}_N : \lambda(p, \mathcal{G}) = \{0\}\}$ .

Following Schmitz et al. [4], in this work we refer to Pauli tableaux as *Pauli frames* to emphasize the linear algebraic structure they represent for the Pauli space.

**Definition 2.** A Pauli frame  $F$  on  $N$  qubits is an  $N \times 2$  array of Hermitian Pauli operators,

$$F = \begin{pmatrix} \text{eff}Z_0 & \text{eff}X_0 \\ \text{eff}Z_1 & \text{eff}X_1 \\ \vdots & \vdots \\ \text{eff}Z_{N-1} & \text{eff}X_{N-1} \end{pmatrix}, \quad (3)$$

which satisfy the following commutation relations:

$$\lambda(\text{eff}Z_i, \text{eff}Z_j) = \lambda(\text{eff}X_i, \text{eff}X_j) = 0 \quad (4a)$$

$$\lambda(\text{eff}Z_i, \text{eff}X_j) = \delta_{ij}. \quad (4b)$$

We also define  $\text{eff}Y_i = -i\text{eff}Z_i * \text{eff}X_i$  and the *origin* frame  $F^0$  such that  $\text{eff}\sigma_i = \sigma_i$  for all  $i$ . Furthermore, we say a Pauli  $P \in \mathcal{G}_N$  is *in the frame* ( $\epsilon$ )  $F$  if there exists an index  $0 \leq i < N$  such that  $P = \text{eff}X_i$ ,  $P = \text{eff}Y_i$  or  $P = \text{eff}Z_i$ .

An extensive discussion on the understanding of Pauli frames as Clifford unitaries can be found in [1]. Instead, we focus our discussion here on Pauli frame as a representation of a *symplectic automorphism* on the Pauli space. A symplectic automorphism on  $(\mathcal{P}_N, \lambda)$  is any linear map  $f : \mathcal{P}_N \rightarrow \mathcal{P}_N$  which preserves the symplectic form.<sup>4</sup> Given a Pauli frame as defined in Eq.(3), one can lift it to two symplectic automorphism defined by

$$\vec{F}(p) = \sum_i (\lambda(p, [X_i])[\text{eff}Z_i] + \lambda(p, [Z_i])[\text{eff}X_i]), \quad (5a)$$

$$\overleftarrow{F}(p) = \sum_i (\lambda(p, [\text{eff}X_i])[Z_i] + \lambda(p, [\text{eff}Z_i])[X_i]). \quad (5b)$$

Furthermore, we use the term *frame*[23] as it emphasizes the following linear algebraic properties. It should be obvious from the commutation relations  $F$  satisfies that  $\vec{F}([Z_i]) = [\text{eff}Z_i]$  and  $\vec{F}([X_i]) = [\text{eff}X_i]$ .  $F^0$  is clearly lifted to a basis for  $\mathcal{P}_N$ , which implies that elements of  $F$  are also lifted to a basis via the expansion of any  $p \in \mathcal{P}_N$ ,

$$p = \sum_i (\lambda(p, [\text{eff}X_i])[\text{eff}Z_i] + \lambda(p, [\text{eff}Z_i])[\text{eff}X_i]). \quad (6)$$

So we can interpret a Pauli frame in this context as both a basis for  $\mathcal{P}_N$  as a symplectic frame as well as a symplectic automorphism. From this and Eq. (6), it is clear that  $\overleftarrow{F} = (\vec{F})^{-1}$ .<sup>5</sup> It should also be clear that any symplectic automorphism,  $f$  can be interpreted as a canonically positive Pauli frame via  $F = \{(f([Z_i]), f([X_i]))\}_{0 \leq i < N}$  and thus can be mapped to a Clifford unitary.<sup>6</sup> It can also be shown that any set of

<sup>4</sup>For all  $p, q \in \mathcal{P}_N$ ,  $\lambda(f(p), f(q)) = \lambda(p, q)$ . Some immediate consequences of this definition and the properties of  $\lambda$  are that  $f^{-1}$  exists and  $\lambda(f(p), q) = \lambda(p, f^{-1}(q))$ .

<sup>5</sup>This provides a means for inverting a signed Pauli frame and thus the Clifford unitary it represents by asserting the signs of  $F^{-1}$  are such that  $\vec{F}(F^{-1}) = F^0$ .

<sup>6</sup>More accurately, the set of symplectic automorphisms is isomorphic to the Clifford group quotient the Pauli group, and we are arbitrarily using canonical positivity of the elements as a means of select an element from each equivalence class of the quotient group.

$2N$  members of  $\mathcal{P}_N$  when divided into two groups forms a symplectic frame, i.e. can be mapped to a Clifford unitary, if and only if they satisfy the commutation relations in Eqs.(4). Importantly, linear independence in such a set is implied by the commutation relations. In fact, a corollary to this result is any set of such pairs of elements of  $\mathcal{P}_N$  less than  $N$  must also be linearly independent.

#### D. The PCOAST Graph and its Semantics

The primary representation which we consider optimizing is the *PCOAST graph*. In particular, we assume a *frame-terminating, fully-merged* PCOAST graph as described in Ref. [1]. We leave a detailed discussion of the process of converting to the PCOAST graph representation and synthesis back to a circuit representation to the reference, but give a brief overview of the structure of the PCOAST graph representation here.

A PCOAST graph is a representation of a generic quantum program which can be described as a sequence of gate-like channels represented as nodes. We use the notation  $\llbracket \cdot \rrbracket$  when interpreting a formal node or collection of them called a *term* as a channel, where

$$\llbracket t_1; t_2 \rrbracket = \llbracket t_2 \rrbracket \circ \llbracket t_1 \rrbracket. \quad (7)$$

The direct equivalence between interpreted terms is referred to as *hold equivalence*,  $\equiv^{\text{hold}}$ , which is contrasted with *release equivalence*, denoted  $\equiv^{\text{release}}$ , when the interpreted terms both satisfy Defn. 1. The sequencing of constituent nodes of a term is then encoded in a directed acyclic graph (DAG) where nodes are non-Clifford unitary and non-unitary quantum channels. A *singlet node* is any node defined by a single Pauli operator  $P$  as represented by  $n(P)$ . This includes  $\text{Rot}(P, \theta)$  which represents a Pauli rotation around the axis  $P$  by an angle of  $\theta/2$  and  $\text{Meas}^c(P)$  which represents a projective measurement of the eigenvalues of  $P$  where the outcome is recorded to classical variable  $c$ . A *factor node* is any node defined by a pair of non-commuting Pauli operators  $(P, Q)$  as represented by  $n(P, Q)$ . This includes  $\text{Prep}(P, Q)$  which represents a preparation or reset of the state to the  $+1$  eigenspace of  $P$  using  $Q$  as conditional operation to take the state out of the  $-1$  eigenspace. Other single qubit rotations can be generalized as factor nodes, but we avoid discussing them here for clarity. Non-classical nodes are also included for mapping measurement outcomes.

Edges are drawn in the graph based on non-commutativity of the defining Pauli operators with the direction of the edge determined by the logical order of operation for the quantum channel it represents. Thus any topological sort of the DAG results in the same overall channel. The assumption of being *fully-merged* means all nodes satisfying the merging rules found in [1] are merged so long as they are not path-connected or *incomparable*. A PCOAST graph is *frame terminating* when it contains a single Pauli frame node representing a residual Clifford unitary channel to be applied last. As discussed in [1], any PCOAST graph can be reduced to this form and the

semantics of frames is such that for any Pauli operator  $P \in \mathcal{G}_N$  and terminating frame  $F$ ,

$$\llbracket U^F \rrbracket(P) = \llbracket F \rrbracket(P) = \overleftarrow{F}(P). \quad (8)$$

This also implies that

$$\llbracket F_1; F_2 \rrbracket = \llbracket F_1 \circ F_2 \rrbracket \quad (9)$$

where we define  $F_1 \circ F_2 = \overrightarrow{F}_1 \circ \overrightarrow{F}_2(F_0) = \overrightarrow{F}_1(F_2)$ .<sup>7</sup>

#### IV. STABILIZER SEARCH

Several of the optimizations we describe below depend on an algorithmic solution to the following problem:

**Definition 3.** (*Stabilizer search problem*) Let  $S$  be a mutually-commuting (Hermitian) subset of  $\mathcal{G}_N - \mathbb{Z}_2$ . The span of  $S$  forms the *stabilizer subspace*,  $\text{Span}(S) = \mathcal{G}_S \subset \mathcal{P}_N$ . Given some cost metric on Pauli frames (namely cost to implement as a circuit), find a low cost frame,  $F$ , for which there exists a similar mutually commuting set  $S'$  such that  $S' \subset F$  and  $\mathcal{G}_S \subseteq \text{Span}(S') = \mathcal{G}_{S'}$ . If we require  $\mathcal{G}_S = \mathcal{G}_{S'}$ , we refer to it as the *exact stabilizer search problem*.

The primary use case for this problem is to measure a set of mutually commuting Pauli operators using the fewest resources as discussed in Section II. Deriving our solution to this problem is an interesting exercise in leveraging the symplectic vector space formalism. For brevity, we provide an overview of the key insights from such a derivation along with a proof of its correctness as a solution.

The power of couching the problem in the language of linear algebra is that we have a well-understood analog from which to draw intuition. As we generally expect the initial set  $S$  to over-determine its span, we can see this problem as a variant of finding the null space or row space of a non-symmetric matrix. In particular, we characterize the null space of the *syndrome map* in the general case or the row space of the *stabilizer map* in the exact case, using the language of quantum error correction[24, 25]. Either way, the solution invokes Gaussian reduction, but with the analogous set of row operations, noting the *two-qubit entangling* (TQE) gates are as outlined in Ref. [4]:<sup>8</sup>

- 1) Row swapping  $\rightarrow$  virtual qubit/Pauli position swapping,
- 2) Row scalar multiplication  $\rightarrow$  nothing as the field is binary,
- 3) In-place row addition  $\rightarrow$  applying a TQE gate.

Thus the algorithm, by virtue of (3), simultaneously produces a circuit which preforms the Clifford transformation. We also note that the process of reducing to row echelon form has the property that the column of the pivot for a reduced row can be effectively ignored from then on. This is analogously handled here by *support masking* provided by the function  $\text{Mask} : \mathcal{G}_N \times (\text{subsets of qubits}) \rightarrow \mathcal{G}_N$ , where

$$\text{Mask}(P, Q) = \text{phase}(P) \prod_{i \in Q} (P)_i. \quad (10)$$

<sup>7</sup>The action is implied to be entry-wise.

<sup>8</sup>For a given qubit pair there are  $3 \times 3 = 9$  TQE gates, generalizing CNOT and CZ, such that we have one Pauli operator basis for each qubit.

```

1: function FINDSTABILIZERS( $S$ , “general” or “exact”)
2:    $S'' \leftarrow S$ ,  $Q \leftarrow \text{supp}(S'')$ ,  $F' \leftarrow F^0$ ,  $C \leftarrow \emptyset$ .
3:   if this is the “general” case then
4:     for  $i \in Q$  do
5:       if  $S''$  agrees on support  $\sigma$  for qubit  $i$  then
6:         Add a measurement for  $\sigma_i$  to  $C$ .
7:         Remove  $i$  from  $Q$ .
8:   while  $Q$  is not empty do
9:     for each  $s \in S''$  do
10:      if  $\text{supp}(\text{Mask}(s, Q))$  is empty then
11:        Remove  $s$  from  $S''$ 
12:      else if  $\text{Mask}(s, Q) = \pm \sigma_i$  for some  $i \in Q$  then
13:        Add measurement of  $\pm \sigma_i$  to  $C$ .
14:        Remove  $i$  from  $Q$ .
15:       $\text{Min} \leftarrow \{\arg \min_{s \in S''} \text{supp}(\text{Mask}(s, Q))\}$ 
16:       $\text{MinGate} \leftarrow \{\text{TQE gates which reduces } \text{supp}(\text{Min})\}$ 
17:       $g_{\min} \leftarrow \arg \min_{g \in \text{MinGate}} \text{Cost}(g)$ 
18:      Add  $g_{\min}$  to  $C$ .
19:       $S'' \leftarrow \overrightarrow{F}_{g_{\min}^{-1}}(S'')$ ,  $F' \leftarrow F_{g_{\min}^{-1}} \circ F'$ .
20:   return  $(C, F'^{-1})$ .

```

Fig. 3: Pseudocode for Stabilizer Search Algorithm.  $\text{Cost}(g)$  is any cost metric on the use of the TQE gate  $g$  for reducing support.

That is, it reduces the support of  $P$  to that which is contained in  $Q$ . One Pauli-space specific consideration is that of *support agreement*:

**Definition 4.** For any mutually commuting set  $S \subset \mathcal{G}_N$ , we say  $S$  agrees on support  $\sigma = X, Y, Z$  for qubit  $i$  iff for every element  $s \in S$ ,  $\lambda(s, \sigma_i) = 0$ . That is, every element of  $S$  either has support  $\sigma$  or no support on  $i$ .

With this concept, we can paraphrase Defn. 3 as the transformation of  $S$  by a Clifford unitary such that every element agrees on support for every qubit. Thus we propose the *Stabilizer Search Algorithm* in Fig. 3, as described for the use of simultaneous measurements.

We defer any discussion around termination of FINDSTABILIZERS to the implementation section below and take for granted that the algorithm terminates. To prove Fig. 3 satisfies Defn. 3, we prove the following:

**Lemma 1.** For  $F$  returned by FINDSTABILIZERS on set  $S$ , the set  $\overrightarrow{F}^{-1}(S)$  agrees on its support for all qubits.

*Proof.* In the general case,  $S$  automatically agrees on all qubits  $i$  which are removed in lines 4-7 of Fig. 3. Otherwise, all qubits are in  $Q$  at the start and  $S$  agrees on all qubit not in  $Q$  vacuously. Then let  $\Delta Q_{\text{init}}$  contain all qubits not in  $Q$ .

For the sake of argument, suppose at step  $m$  and for all  $m' \leq m$  through the main loop of the algorithm,  $\overrightarrow{F}'_{(m')}(S) = S'_{(m')}$  agrees on its support for all qubits not in  $Q_{(m')}$ , where  $(m')$  denotes the  $m^{\text{th}}$  versions of  $F'$ ,  $Q$  and other quantities at the end of that iteration. Now consider the beginning of

the  $(m+1)^{th}$  iteration. At step (1), if  $\text{Mask}(s, Q_{(m)})$ , for  $s \in S'_{(m)} \subseteq S'_{(m)}$ , has no support, then it agrees with the rest of  $S'_{(m)}$  by our hypothesis and is then absent from  $S'_{(m+1)}$ . If  $\text{Mask}(s, Q_{(m)}) = \pm\sigma_q$ , then consider for any  $s' \in S'_{(m)}$ ,

$$\begin{aligned} \lambda(\sigma_q, s') &= \lambda_q(\text{Mask}(s, Q_{(m)}), s') \\ &= \sum_{i \in Q_{(m)}} \lambda_i(s, s') + \sum_{i \notin Q_{(m)}} \lambda_i(s, s') \\ &= \lambda(s, s') = \lambda(\vec{F}_{(m)}^{-1}(s), \vec{F}_{(m)}^{-1}(s')) \\ &= 0. \end{aligned} \quad (11)$$

Eq. 11<sup>9</sup> implies that all of  $S'_{(m)}$  agrees on the support of  $\sigma$  on  $q$  and as we remove it,  $q \notin Q_{(m+1)}$ . Thus by the end of step (1), all changes to  $Q$  are made such that  $Q_{(m)} \rightarrow Q_{(m+1)}$ , and all of  $S'_{(m)}$  agrees on support for all of  $\Delta Q_{(m)} = Q_{(m)} - Q_{(m+1)}$ .

The TQE gate selection in lines 15-17 insures  $g_{\min(m)}$  only acts on elements of  $Q_{(m+1)}$ . Therefore since  $S'_{(m)}$  agree on support for qubits not in  $Q_{(m+1)}$ , it is the case that  $S'_{(m+1)} = \vec{F}_{g_{(m)}^{-1}}(S'_{(m)})$  must also agree on support for qubits not in  $Q_{(m+1)}$ .

Assuming the algorithm terminates, there exists  $M$  such that  $Q = \bigcup_{0 \leq m < M} \Delta Q_{(m)} \cup \Delta Q_{\text{init}}$  and  $F = F_{(M)}^{-1}$ . Therefore by induction, we have that  $\vec{F}^{-1}(S)$  agrees on its support for all qubits.  $\square$

An immediate corollary to this proof is that every measurement in the circuit corresponds to the support agreement for all qubits  $Q$  on which  $S$  has support. Let  $\Sigma = \{\sigma_q\}_{q \in Q}$  be the set of support agreement as found from the returned circuit. As each element of  $\Sigma$  is a single qubit Pauli operator on different qubits, every element of  $S' = \vec{F}(\Sigma)$  belongs to  $F$  and is mutually commuting. To prove this set of operators satisfy Defn. 3, it is sufficient to prove  $S' \subseteq \mathcal{G}_S^\perp$ .<sup>10</sup> But this immediately follows from the above proof since,

$$\lambda(S, S') = \lambda(S, \vec{F}(\Sigma)) = \lambda(\vec{F}^{-1}(S), \Sigma) = \{0\}, \quad (12)$$

Because  $\vec{F}(\Sigma)$  is contained in the frame  $F$ , we can use Eq. 6 to expand members of  $S$  as a product of elements in  $S'$  via the *Map Measurement Algorithm* as described in Fig. 4.<sup>11</sup>

<sup>9</sup>The subscript on  $\lambda$  represents its functional support on that qubit, the first equality is a consequence of  $s$  have single-qubit masked support, the second is a consequence of our induction hypothesis, and the final two equalities are a consequence of the automorphism property of frames and the fact that  $S$  is a mutually commuting set.

<sup>10</sup>This on its own is actually not sufficient. We need to also show that all members of  $S$ , when expanded in the basis  $F$ , contains only terms from elements of  $F$  associated with  $Q$ . However, it should be clear that this is trivially true as  $S$  has no support outside of  $Q$  and the gates used to generate  $F$  and thus by extension  $F$  itself have no action on operators with no support in  $Q$ .

<sup>11</sup>We must address why the exact version of Fig. 3 satisfies the exact condition of Defn. 3. The binary matrix  $\underline{b}$  returned by Algorithm 4, when restricted to elements of  $S$  satisfying line 12 of Fig. 3 has an upper triangular form and is thus inevitable.

```

1: function MAPMEASUREMENTS( $S, C, F$ )
2:    $\Sigma \leftarrow \{\sigma_q\}$ , where each  $\sigma_q$  is a measurement in  $C$ .
3:    $S' \leftarrow \vec{F}(\Sigma)$ ,  $\underline{b} \leftarrow \mathbf{0}$ ,  $v \leftarrow \vec{0}$ .
4:   for all  $s_i \in S$  do
5:     Pauli  $P \leftarrow I$ 
6:     for all  $\sigma_q \in \Sigma$  do
7:       if  $\lambda(s_i, F(\tilde{\sigma}_q))$  then
8:          $P \leftarrow P * F(\sigma_q)$ ,  $\underline{b}_{iq} \leftarrow 1$ .
9:       if  $\text{phase}(P) \neq \text{phase}(s_i)$  then
10:         $v_i \leftarrow 1$ .
11:   return  $(\underline{b}, v)$ 

```

Fig. 4: Pseudocode for Map Measurement Algorithm.

### A. Implementation of the Stabilizer Search Algorithm

It should be clear from the discussion in the Section V.C of Ref. [1] that, given the appropriate *search functions*, the greedy search algorithm for circuit synthesis is well suited for implementing Fig. 3. As argued in [1], we are then guaranteed the algorithm terminates. Moreover we can modify almost any version of the search functions used for circuit synthesis so long as they make an additional promise.<sup>12</sup> Thus we introduce the *stabilizer search template*. This is a templated implementation of the search functions which holds internally a list of qubits for the sake of masking and removes a qubit when a measurement is added to the circuit.

The complexity of Fig. 3 also follows from Ref. [1] as  $\mathcal{O}(N^3 k^2)$  where  $k$  is the size of the outcome stabilizer set  $S'$  which is also its stabilizer space dimension. The number of TQE gates it produces is at most  $Nk - k(k+1)/2$ , but tends toward far lower numbers as we demonstrate in Section VII while also taking into consideration circuit depth and the target gate set.

## V. UNITARY REDUCTION BY PREPARATIONS

### A. Frame Reduction

In this section, we discuss an algorithmic solution to the following problem:

**Definition 5.** (*Preparation-on-frame reduction problem*) Suppose we have a set of mutually commuting, un-equal preparation channels  $\text{Prep}(\{(P_i, Q_i)\}) = \text{Prep}(\Pi)$ , followed by a Clifford unitary channel as defined by the Pauli frame  $F$ . Given some cost metric on Pauli frames (again, typically circuit cost to implement), find a lower cost frame  $F'$  and possibly lower cost representation  $\Pi' = \{(P'_i, Q'_i)\} \simeq \Pi$  such that,

$$\llbracket \text{Prep}(\Pi); F \rrbracket = \llbracket \text{Prep}(\Pi'); F' \rrbracket. \quad (13)$$

For  $\text{Prep}(P, Q)$ , we refer to  $P$  as the *stabilizer*, which is privileged over  $Q$  which we refer to as the *destabilizer*[22]. To understand the preparation-on-frame reduction problem,

<sup>12</sup>REDUCENODE as described in [1] only returns TQE gates entirely supported on the qubit support of the passed node.

we first consider what is meant by  $\Pi \simeq \Pi'$ . As discussed in [1], a pair of anti-commuting Pauli operators can always be understood as defining an effective qubit factorization of the Hilbert space. From the description of  $\text{Prep}$  in Section III-D, we find that  $\Pi$  generalize this such that it defines an effective multi-qubit factorization of the Hilbert space where the outcome of  $\text{Prep}(\Pi)$  is a simultaneous +1 eigenstate of the stabilizers, using a specific combination of destabilizers to transform out of any other alternative stabilizer subspace.<sup>13</sup> Thus  $\text{Prep}(\Pi')$  must have the same action on any state. Finding such an alternative should already evoke the exact version of Defn. 3. Let  $S = \text{Stabs}(\Pi) = \{P_i\}$ , on which we can apply the exact version of Fig. 3 to find  $S' = \text{Stabs}(\Pi')$  and  $F$ . To construct corresponding destabilizers,  $\{Q'_i\}$ , note they must satisfy  $\lambda(P'_i, Q'_i) = \delta_{ij}$  and  $\lambda(Q'_i, Q'_j) = 0$ . For simplicity, assume  $Q'_i \in \text{Span}(\{Q_j\})$  such that the second condition is satisfied. Let  $\tilde{Q}_i \in F$  be one of the two elements which anti-commutes with  $P'_i$ . We then find that,<sup>14</sup>

$$\begin{aligned} [Q'_i] &= \sum_j \lambda(Q'_i, P_j)[Q_j] = \sum_{j,k} \lambda(Q'_i, P'_k) \lambda(\tilde{Q}_k, P_j)[Q_j] \\ &= \sum_j \lambda(\tilde{Q}_i, P_j)[Q_j], \end{aligned} \quad (14)$$

We also consider the equivalence in Eq. (13). An alternative formulation of  $\llbracket \text{Prep}(\Pi) \rrbracket$  is as a partial trace over the subsystem/factor defined by  $\Pi$ , tensor product with the projection onto the appropriate stabilizer subspace, i.e.

$$\llbracket \text{Prep}(\Pi) \rrbracket(\rho) = \text{Tr}_{\Pi}(\rho) \otimes \text{Proj}(S), \quad (15)$$

where  $\text{Proj}(S)$  is defined as the projection onto the simultaneous +1 stabilizer space of  $S$ . From this, it is clear that when  $\rho$  is expanded in the Pauli operator basis, terms not wholly outside of the subsystem defined by  $\Pi$  are zero under the partial trace and all remaining terms are multiplied in equal measure by elements from  $\text{Span}(S)$ . Thus the frames  $F$  and  $F'$  in Eq. (13) need only have the same action on this limited set of Pauli operators. This provides us with the following conditions:

**Lemma 2.** *Eq. (13) is true if and only if<sup>15</sup>*

$$\overleftarrow{F}(\text{Span}(S)) \simeq \overleftarrow{F}'(\text{Span}(S)), \quad (16a)$$

$$\frac{\overleftarrow{F}(\text{Span}(\Pi)^\perp \oplus \text{Span}(S))}{\text{Span}(S)} = \frac{\overleftarrow{F}'(\text{Span}(\Pi)^\perp \oplus \text{Span}(S))}{\text{Span}(S)} \quad (16b)$$

The first says that  $F$  can modify the stabilizers over what  $F'$  does, but it must preserve the space.<sup>16</sup> The second condition

<sup>13</sup>Alternatively, we understand equivalence by considering a symplectic subspace of  $\mathcal{P}_N$  with symplectic form provided by  $\lambda$  as restricted to that subspace, for which  $\Pi$  is a frame for that subspace and can be used as such.  $\Pi'$  is then just an alternate frame for that subspace.

<sup>14</sup>Note that we can freely ignore sign here, because the sign of a destabilizer does not change the channel action.

<sup>15</sup>Note,  $s \in \text{Span}(S)$ ,  $s\text{Proj}(S) = \text{Proj}(S)$ , i.e. the projection operator can always absorb a stabilizer. This is necessary for understanding Eq.16b.

<sup>16</sup>Though we are using the language of the Pauli space here, it is fundamental that the signs are also preserved by  $F$  as well.

is more strict with the exact equality implying that any Pauli operator which commutes with all of the elements of  $\Pi$  must be transformed exactly the same by  $F$  and  $F'$  modulo some element of  $\text{Span}(S)$ .

This leads us to introduce a frame transformation we refer to as *qubit decoupling*:

**Definition 6.** For an anti-commuting pair  $(P, Q)$  and frame  $F$  as defined in Eq. 3 such that  $P \in F$ , the qubit decoupling transformation  $\text{Decouple}(F, (P, Q))$  is defined as

$$\begin{pmatrix} \text{eff}Z_0 P^{\lambda(\text{eff}Z_0, Q)} & \text{eff}X_0 P^{\lambda(\text{eff}X_0, Q)} \\ \text{eff}Z_1 P^{\lambda(\text{eff}Z_1, Q)} & \text{eff}X_1 P^{\lambda(\text{eff}X_1, Q)} \\ \vdots & \vdots \\ P & Q \\ \vdots & \vdots \\ \text{eff}Z_{N-1} P^{\lambda(\text{eff}Z_{N-1}, Q)} & \text{eff}X_{N-1} P^{\lambda(\text{eff}X_{N-1}, Q)} \end{pmatrix}. \quad (17)$$

At times we omit the argument  $(P, Q)$  for brevity. To show  $\text{Decouple}$  results in a valid frame, note  $P$  was a part of  $F$  and has all the correct commutation relation with respect to the other elements of the resultant frame. Likewise is true for those elements multiplied by it. The only commutation relations of interest involve  $Q$  for which,

$$\begin{aligned} \lambda(Q, \text{eff}Z_i P^{\lambda(\text{eff}Z_i, Q)}) &= \lambda(Q, \text{eff}Z_i) + \lambda(P, Q) \lambda(\text{eff}Z_i, Q) \\ &= 0 \end{aligned} \quad (18)$$

Next we show the transform  $\text{Decouple}$  preserves the properties of Lemma 2. Since  $P$  is a member of the frame, Eq. (16a) is satisfied trivially. Without loss of generality, suppose  $P$  is  $\text{eff}Z_q$  and consider  $r \in \mathcal{P}_N$  such that  $\lambda(P, r) = \lambda(Q, r) = 0$ . Note this implies for  $i \neq q$   $\lambda(r, \text{eff}Z_i P) = \lambda(r, \text{eff}Z_i)$ , and likewise for  $\text{eff}X_i$ . Thus we find,

$$\llbracket \llbracket \text{Decouple}(F) \rrbracket(r) \rrbracket = \llbracket \llbracket F \rrbracket(r) \rrbracket + \lambda(r, \text{eff}X_q)[P]. \quad (19)$$

Therefore,  $\text{Decouple}$  also satisfies Eq. (16b).

$\text{Decouple}$  is a powerful tool for reducing the cost of a frame in the presence of a single  $\text{Prep}$ , but requires the stabilizer to be a part of the frame. To generalize, we find an auxiliary frame,  $F_{\text{aux}}$  such that  $F \circ F_{\text{aux}}$  does contain the stabilizer. As such  $F' = \text{Decouple}(F \circ F_{\text{aux}}) \circ F_{\text{aux}}^{-1}$ , satisfies Eq. (16). This processes is then generalized  $\Pi$  or alternatively  $\Pi'$ . For this purpose, we introduce the *Preparation-on-Frame Reduction Algorithm* in Fig. 5. The correctness of Fig. 5 can then be argued with the following lemma:

**Lemma 3.** *Every call to  $\text{Decouple}$  in Fig. 5 is well-formed.*

*Proof.* Suppose Fig. 5 enters the first branch at line 7. By construction, for each  $\sigma_{q_i}$ ,  $\overleftarrow{F} \circ F_{\text{aux}}(\sigma_{q_i}) = P'_i$  is both in the frame  $F \circ F_{\text{aux}}$ , and a stabilizer of  $\Pi'$ . Also, the outcome of  $\text{Decouple}(F \circ F_{\text{aux}}, (P'_i, Q'_i))$  contains  $P'_j$  for any  $j \neq i$ , since  $\lambda(P'_j, Q'_i) = 0$ . Therefore the decoupling sequence is well-formed.

```

1: function REDUCEFRAMEBYPREP( $\Pi, F$ )
2:    $S \leftarrow \text{Stabs}(\Pi)$ ,  $M \leftarrow |S|$ ,  $\tilde{S} \leftarrow \overleftarrow{F}(S)$ 
3:    $(C, F_{\text{aux}}) \leftarrow \text{FINDSTABILIZERS}(\tilde{S}, \text{"exact"})$ .
4:   Let  $\{\sigma_{q_i}\}_{0 \leq i < M}$  be the measurements in order from  $C$ .
5:   Construct  $\Pi'$  using  $\Pi$ ,  $F \circ F_{\text{aux}}$  and Eq. (14).
6:    $c \leftarrow \text{Cost}(\Pi)$ ,  $c' \leftarrow \text{Cost}(\Pi')$ 
7:   if  $c' < c$  then
8:      $\tilde{F} \leftarrow \text{Decouple}(F \circ F_{\text{aux}}, \Pi')$   $\triangleright$  in any order
9:     return  $(\Pi', \tilde{F} \circ F_{\text{aux}}^{-1})$ .
10:  else
11:     $\tilde{F}_0 \leftarrow F \circ F_{\text{aux}}$ .
12:    for  $i = 0$  up to  $M$  do
13:      Let  $(P_i, Q_i) \in \Pi$  such that  $P_i = \overleftarrow{F}_i(\sigma_{q_i})$ .
14:       $\tilde{F}_{i+1} \leftarrow \text{Decouple}(\tilde{F}_i, (P_i, Q_i))$ 
15:    return  $(\Pi, \tilde{F}_M \circ F_{\text{aux}}^{-1})$ 

```

Fig. 5: Pseudocode for Preparation-on-Frame Reduction Algorithm.  $\text{Cost}(\Pi)$  represents some cost evaluation for implementing of  $\text{Prep}(\Pi)$ .

Alternatively, suppose Fig. 5 enters the else branch at line 10. Note, as a property of using of the exact version of Fig. 3, we have that for all  $m < M$

$$\overleftarrow{F}_0^{-1}(P_m) = \sigma_{q_m} + \sum_{i < m} c_{mi} \sigma_{q_i}, \quad (20)$$

where  $c_{mi}$  is some binary scalar and  $P_m$  is the  $m^{\text{th}}$  element of  $\text{Stabs}(\Pi)$  which was reduced to support 1 when masked in the call at line 3. In the first step of the loop, It is clear from Eq. (20), that  $\overleftarrow{F}_0(\sigma_{q_0}) = P_0 \in \Pi$ . Thus the first **Decouple** is well-formed.

For the sake of argument, now assume that for all  $m' < m$ , where  $m < M$ , the  $m^{\text{th}}$  **Decouple** was well-formed. Now consider the  $m^{\text{th}}$  step and  $\overleftarrow{F}_m(\sigma_{q_m}) \in \tilde{F}_m$  which, based on our hypothesis and the definition of **Decouple** can be written as,

$$\overleftarrow{F}_m(\sigma_{q_m}) = \overleftarrow{F}_0(\sigma_{q_m}) + \sum_{m' < m} \lambda(\overleftarrow{F}_0(\sigma_{q_m}), Q_{m'}) P_{m'} \quad (21)$$

where we note that because  $\overleftarrow{F}_0(\sigma_{q_m}) \in \text{Span}(\Pi)$ , we can expand it in  $\Pi$  as a basis, noting  $\lambda(\overleftarrow{F}_0(\sigma_{q_m}), P_{m'}) = 0$ :

$$\begin{aligned} \overleftarrow{F}_0(\sigma_{q_m}) &= \sum_{m' < M} \lambda(\overleftarrow{F}_0(\sigma_{q_m}), Q_{m'}) P_{m'} \\ &= P_m + \sum_{m' < m} \lambda(\overleftarrow{F}_0(\sigma_{q_m}), Q_{m'}) P_{m'}, \end{aligned} \quad (22)$$

where the last equality is a consequence of inverting the upper triangular form of Eq. (20) and the uniqueness of the expansion in this basis. From this it immediately follows  $\overleftarrow{F}_m(\sigma_{q_m}) = P_m$  and thus the **Decouple** for this step is well formed and by induction the sequence of **Decouples** is well-formed.  $\square$

```

1: function REDUCENODESBYPREP( $G$ )
2:    $G' \leftarrow G$ ,  $\text{Prep}(G') \leftarrow$  all Prep nodes in  $G'$ .
3:   for  $n = n(P, Q) \in \text{Prep}(G')$  do
4:     for  $n'(R)$  incomparable of  $n$ ,  $n' \notin \text{Prep}(G')$  do
5:       if  $\text{Cost}(n'(R * P)) < \text{Cost}(n'(R))$  then
6:          $R \leftarrow R * P$  such that  $n'$  comes after  $n$ .
7:       for  $n(R)$  distance +1 from  $n$ ,  $\lambda(P, R) = 0$  do
8:         if  $\text{Cost}(n(R * P)) < \text{Cost}(n(R))$  then
9:           Replace  $n(R)$  with  $n(R * P)$ .
10:        else if  $n(R * P)$  or can be merged in  $G'$  then
11:          Replace  $n(R)$  with  $n(R * P)$ .
12:   return  $G'$ .

```

Fig. 6: Pseudocode for Preparation-on-Node Reduction Algorithm.

### B. Non-Clifford Reduction

Non-Clifford nodes of the PCOAST graph can also be simplified when “seen” by a  $\text{Prep}(P, Q)$ . As demonstrated in Eq. (15),  $P \sim I$  after the application of  $\text{Prep}(P, Q)$ . Thus for a singlet node dependent on the Pauli operator  $R$ ,  $n(R)$ , which is incomparable with  $\text{Prep}(P, Q)$ , we have that

$$\begin{aligned} \llbracket n(R); \text{Prep}(P, Q) \rrbracket &= \llbracket \text{Prep}(P, Q); n(R) \rrbracket \\ &= \llbracket \text{Prep}(P, Q); n(P * R) \rrbracket. \end{aligned} \quad (23)$$

Note this relation goes both ways. We can also consider applying this identity to a node defined by  $R' = R * P$ , i.e.  $\lambda(R'P) = 0$  and  $\lambda(R', Q) = 1$ . Which version we choose for the sake of optimization depends on the cost of the outcome. We thus outline the use of Eq. (23) for the *Preparation-on-Node Reduction Algorithm* in Fig. 6.<sup>17</sup>

## VI. PCOAST GRAPH OPTIMIZATIONS

The previous sections outline the tools we leverage for PCOAST graph optimization. The full sequence of the *PCOAST Graph Optimization Algorithm* is described in Fig. 7. Note the conditional introduced at line 13 is added specifically to target cases similar to Fig. 1d.

While Fig. 7 is used to optimize the PCOAST graph back to another PCOAST graph, there are other uses of the routines described herein. During circuit synthesis as described in [1], the synthesis of non-Clifford nodes intentionally defers synthesis of measurement nodes topologically at the end of the graph in the “release” case and returns them. Note these nodes are clearly mutually commuting and so we are free to use Fig. 3 to synthesize the remaining circuit and Fig. 4 for the mapping of measurements. A benefit of this methodology is the stabilizer search is performed in the “context” of the rest of the circuit since the measurements are transformed by the residual Clifford. For example, consider the case of a VQE algorithm circuit where one first prepares an ansatz state and then measures part of the Hamiltonian using a mutually commuting set. The stabilizer search of the mutually

<sup>17</sup>Note we only check for node merging in line 10 and not earlier as to do so would be redundant by Eq.(23).

```

1: function OPTIMIZEGRAPH( $G, F$ , “hold” or “release”)
2:    $G' = \emptyset$ , and  $G'' \leftarrow G$ .
3:   while  $G' \neq G''$  do
4:      $G' \leftarrow \text{REDUCENODESBYPREP}(G'')$ 
5:   Let  $\Pi_e$  be the set of Prep nodes with outdegree 0.
6:   if this is the “hold” case then
7:      $(\Pi_e, F) \leftarrow \text{REDUCEFRAMEBYPREP}(\Pi_e, F)$ .
8:   else if this is the “release” case then
9:     Let  $M_e$  be all Meas nodes with outdegree 0.
10:    Let  $C_e$  be the measurement space of  $M_e$ .
11:    Remove all incomparable nodes of  $M_e$  in  $G'$ .
12:     $F \leftarrow F^0$  in  $G'$ .
13:    if  $\Pi_e \neq \emptyset$  then
14:      Let  $C_e$  be the measurement space of  $M_e$ .
15:      Remove  $M_e$  from  $G'$ .
16:       $(F_s, C) \leftarrow \text{FINDSTABILIZERS}(M_e)$ .
17:      Let  $M_n$  be the single-qubit Meas from  $C$ .
18:      Let  $C_n$  be the measurement space of  $M_n$ .
19:       $(\Pi_e, F) \leftarrow \text{REDUCEFRAMEBYPREP}(\Pi_e, F_s)$ .
20:      Add  $M_n$  to  $G'$ .
21:       $(\underline{b}, v) \leftarrow \text{MAPMEASUREMENTS}(M_e, C, F_n)$ 
22:      Add the node  $(v + \underline{b}) : C_n \rightarrow C_e$  to  $G'$ .
23:   return  $G'$ 

```

Fig. 7: PCOAST Graph Optimization Algorithm

commuting measurements in isolation is different than that of the search when combined with the (incomplete) circuit synthesis of the ansatz. As such, its not simply that we optimize the Clifford circuit at the interface of the ansatz preparation and the measurements, but the combined effect may change what Pauli operators are measured to build the desired outcome. We demonstrate this point in Fig. 8 and in the results of Section VII.

## VII. EVALUATION

We focus on the VQE use case and the use of Fig. 3 for measurement reduction. For comparison, we consider three methods found in the literature for solving a similar problem.<sup>18</sup> Ref. [5] only considers the case of qubit-wise commutativity i.e. full qubit agreement as defined in Defn. 4. By virtue of the initial search for agreement in lines 4-7, Fig. 3 produces essentially the same circuit under these circumstances, thus making a direct comparison unnecessary. Ref. [6] allows for general commutativity, but their code implementation requires the commuting set have exactly  $N$  independent elements (whereas our implementation allows one to specify any commuting set without considering independence). They also map the elements of the set, under conjugation by a Clifford, exactly to a single-qubit measurement, i.e. they do not leverage smaller weight bases for the stabilizer space. Ref. [7] is the least

<sup>18</sup>Unlike the references to follow, we only focus on the circuit generation, not the grouping problem for which they provide methods which are fully compatible with this work as demonstrated by our use of the grouping method described in Ref. [7].

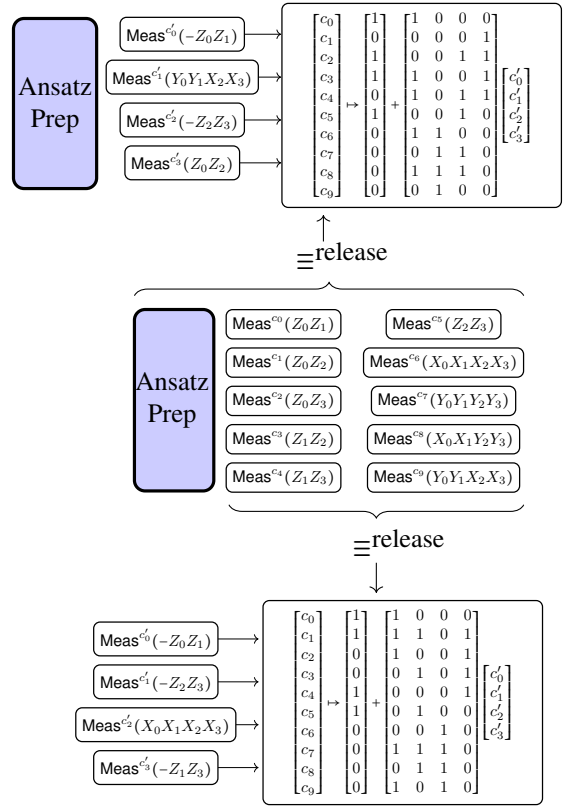


Fig. 8: PCOAST graph representations for a hydrogen VQE example ( $H_2$ ; JW encoding). The center graph represents the ansatz preparation and measurement of one mutually commuting set. The graph below represents the stabilizer search result for the measurements alone, whereas the top result represents the stabilizer search result in the context of the ansatz. Table III demonstrates the top outcome results in a better circuit.

constrained and as such represents the best comparison to our methods; we use their method, SORTED INSERTION, for partitioning the Hamiltonian, and compare PCOAST circuit constructions against their method. Their methods achieve a ratio of the theoretical maximum number of two-qubit gates to actual number of two-qubit gates of approximately 3.5. Thus we compute a similar metric,

$$r_{2q} = \frac{Nk - k(k+1)/2}{\# \text{ 2q gates}}, \quad (24)$$

where  $k$  is extracted as the number of single-qubit measurements in the PCOAST-optimized circuit.

PCOAST is implemented in C++ as the core optimization of the Intel<sup>®</sup> Quantum SDK, enabled by the (-O1) flag, which we use for all our experiments. We apply PCOAST to the Hamiltonians of several molecules in the context of VQE. We use Qiskit’s PySCF driver [26, 27] to express all fermionic Hamiltonians in the STO-3G basis as qubit observables using either the Bravyi-Kitaev (BK) [28] or Jordan-Wigner (JW) [29] transformation. Grouping of the Hamiltonian terms in mutually commuting sets is obtained by using an adapted version of the

TABLE II: Statistics for the measurement circuits for each molecule for both BK and JW mappings.

Benchmark	# Qubits	# Measurements	# Groupings	Avg total gates		Avg 2Q gates		Avg Depth		Avg $r_{2q}$		Avg $k$	
				BK	JW	BK	JW	BK	JW	BK	JW	BK	JW
H <sub>2</sub>	4	15	2	5.00	12.00	0.00	2.50	1.50	4.50	-	2.40	4.00	3.50
HF	12	631	38	41.61	38.34	9.79	8.89	10.53	7.89	6.53	7.12	10.26	9.82
LiH	12	631	41	38.07	36.34	8.27	8.34	9.41	8.15	7.76	7.24	10.46	9.54
BeH <sub>2</sub>	14	666	36	47.33	43.83	11.47	10.36	11.17	9.69	7.53	8.40	11.31	11.31
H <sub>2</sub> O	14	1086	50	48.98	46.88	11.52	11.46	10.76	9.78	7.65	7.58	11.98	11.36
BH <sub>3</sub>	16	1957	76	48.85	53.15	10.29	13.11	10.45	10.03	11.47	8.93	14.40	13.57
NH <sub>3</sub>	16	2949	105	52.28	55.48	11.26	13.64	10.68	10.50	10.54	8.60	14.51	13.82
CH <sub>4</sub>	18	6892	163	71.14	59.24	17.58	13.58	13.89	9.54	8.60	11.04	16.74	16.06
B <sub>2</sub>	20	2239	64	84.96	72.70	23.94	20.23	16.00	13.06	6.31	7.42	16.64	16.26
O <sub>2</sub>	20	2239	67	85.89	72.84	24.57	20.16	15.55	12.95	7.46	9.04	16.43	16.18
Be <sub>2</sub>	20	2951	74	89.56	78.67	24.98	22.16	16.10	14.06	7.42	8.40	17.13	16.95
C <sub>2</sub>	20	2951	75	90.34	78.06	25.36	21.83	15.97	13.55	7.23	8.51	17.28	17.24
F <sub>2</sub>	20	2951	76	88.66	77.15	25.09	22.06	16.57	13.95	7.36	8.32	16.86	16.42
Li <sub>2</sub>	20	2951	78	90.81	77.22	25.87	21.96	17.04	13.67	7.12	8.40	16.87	16.58
N <sub>2</sub>	20	2951	79	93.53	79.00	27.10	22.10	16.90	13.91	6.86	8.41	17.35	17.06

TABLE III: Average (%) reductions in total gate count, two-qubit gates, depth, and measurement gates achieved when PCOAST synthesizes a combined ansatz and measurement circuit vs each individually. Results are shown for both BK and JW mappings.

Benchmark	Total Gates		2Q Gates		Depth		Meas	
	BK	JW	BK	JW	BK	JW	BK	JW
H <sub>2</sub>	70.00	35.27	0.00	41.34	50.00	5.45	75.00	-16.67
HF	5.89	11.54	3.92	10.64	3.89	6.56	7.11	3.62
LiH	5.19	0.93	5.12	-0.72	2.01	0.34	1.63	3.03
BeH <sub>2</sub>	1.90	3.99	0.62	2.69	1.75	0.64	2.91	-7.25
H <sub>2</sub> O	2.81	5.19	2.52	4.33	4.26	2.18	3.55	0.62
CH <sub>4</sub>	4.09	3.16	3.84	2.97	1.04	0.32	1.04	-1.70

SORTED INSERTION algorithm of Ref. [7]. For all benchmarks in Table III, we pick the Unitary Coupled-Cluster Single and Double excitations (UCCSD) [30] as our ansatz. Our experiments use an Intel Xeon® Platinum CPU (2.4GHz, 2TB RAM). All averages are over the various groupings.

Table II shows our results. We find a combined average  $r_{2q}$  value over all benchmarks of 7.85 (7.99) with a maximum value of 11.47 (11.04) for the BK (JW) encoding. All metrics appear to scale linearly in qubit number including  $k$  with the ratio  $\frac{k}{N}$  an average value of 83.64%. It is worth noting that in a majority of benchmarks, the JW encoding outperforms the BK encoding.

We also consider the outcome of synthesizing the measurement circuit collectively with the ansatz using PCOAST. Table III shows the average reductions gained when PCOAST synthesizes a quantum program comprised of both ansatz and measurement circuits vs. when it synthesizes each part individually. Overall, we see that when combined, PCOAST further reduces the total gates, two-qubit gates, depth, and measurement gates by 14.98% (10.01%), 2.67% (10.21%), 10.49% (2.58%), and 15.21% (-3.06%) for the BK (JW) encoding.

Though there is a reduction in aggregate, we find several instances where the separate synthesis outperforms the combined synthesis. Because the separate synthesis outcome is theoretically achievable with the combined synthesis, this

demonstrates that there is more refinement available to both PCOAST in general and the Stabilizer Search Algorithm in particular.

### VIII. CONCLUSION

In this paper, we have introduced a set of optimization routines included in PCOAST which optimize at the interface between unitary and non-unitary operations. This includes reduction of node cost and node number in the presence of preparation nodes via the Preparation-on-Node Reduction Algorithm, reduction of cost for Clifford operations in the presence of preparations via the Preparation-on-Frame Reduction Algorithm, and measurement cost reduction using Clifford operations via the Stabilizer Search Algorithm and the classical remapping of measurement outcomes via the Map Measurement Algorithms. These routines are also combined to amplify their effectiveness when optimizing the PCOAST graph via the PCOAST Graph Optimization Algorithm. These routines were described in detail and shown to be valid relative to the appropriate equivalence (“hold” or “release”). We numerically studied the effectiveness of the Stabilizer Search Algorithm as used for measurement reduction circuits for VQE. We found an overall average ratio of the theoretical maximum number of two-qubit gates to resulting number of two-qubit gates of 7.85 (7.99) for the BK (JW) encoding. We also showed that synthesis of the VQE ansatz along with the measurements results in a better aggregate circuit.

In future work, we hope to further refine the algorithms presented here. In particular, we hope to increase the efficiency of the general Stabilizer Search Algorithm by considering *partial* qubit masking. Instead of a fully opaque qubit mask as defined in Eq.(10), we can weight the cost of the support based on the fraction of measurement elements which don’t agree on that support. This should further reduce the number of TQE gates needed to find full qubit support agreement within the measurement set. We also look to expand the types of optimization routines within PCOAST, including more sophisticated transformations on unitary elements, and better use of stabilizer subspace methods by finding incomparable node cliques in the PCOAST graph.

## REFERENCES

- [1] J. Paykin, A. T. Schmitz, M. Ibrahim, X.-C. Wu, and A. Y. Matsuura, “PCOAST: A Pauli-based quantum circuit optimization framework (extended version),” 2023. [Online]. Available: <https://arxiv.org/abs/2305.10966v2>
- [2] F. Zhang and J. Chen, “Optimizing T gates in Clifford+T circuit as  $\pi/4$  rotations around Paulis,” 2019.
- [3] A. Cowtan, S. Dilkes, R. Duncan, W. Simmons, and S. Sivarajah, “Phase gadget synthesis for shallow circuits,” in *16th International Conference on Quantum Physics and Logic 2019*. Open Publishing Association, 2019, pp. 213–228.
- [4] A. T. Schmitz, N. P. D. Sawaya, S. Johri, and A. Y. Matsuura, “Graph optimization perspective for low-depth Trotter-Suzuki decomposition,” 2021. [Online]. Available: <https://arxiv.org/abs/2103.08602>
- [5] V. Verteletskyi, T.-C. Yen, and A. F. Izmaylov, “Measurement optimization in the variational quantum eigensolver using a minimum clique cover,” *The Journal of Chemical Physics*, vol. 152, no. 12, 03 2020, 124114. [Online]. Available: <https://doi.org/10.1063/1.5141458>
- [6] P. Gokhale, O. Angiuli, Y. Ding, K. Gui, T. Tomesh, M. Suchara, M. Martonosi, and F. T. Chong, “ $o(n^3)$  measurement cost for variational quantum eigensolver on molecular hamiltonians,” *IEEE Transactions on Quantum Engineering*, vol. 1, pp. 1–24, 2020.
- [7] O. Crawford, B. van Straaten, D. Wang, T. Parks, E. Campbell, and S. Brierley, “Efficient quantum measurement of pauli operators in the presence of finite sampling error,” *Quantum*, vol. 51, 2021.
- [8] P. Khalate, X.-C. Wu, S. Premaratne, J. Hogaboam, A. Holmes, A. Schmitz, G. G. Guerreschi, X. Zou, and A. Y. Matsuura, “An LLVM-based C++ compiler toolchain for variational hybrid quantum-classical algorithms and quantum accelerators,” 2022. [Online]. Available: <https://arxiv.org/abs/2202.11142>
- [9] A. Peruzzo, J. McClean, P. Shadbolt, M.-H. Yung, X.-Q. Zhou, P. J. Love, A. Aspuru-Guzik, and J. L. O’Brien, “A variational eigenvalue solver on a photonic quantum processor,” *Nature Communications*, vol. 5, no. 1, jul 2014. [Online]. Available: <https://doi.org/10.1038/ncomms5213>
- [10] K. Bharti, A. Cervera-Lierta, T. H. Kyaw, T. Haug, S. Alperin-Lea, A. Anand, M. Degroote, H. Heimonen, J. S. Kottmann, T. Menke, W.-K. Mok, S. Sim, L.-C. Kwek, and A. Aspuru-Guzik, “Noisy intermediate-scale quantum algorithms,” *Rev. Mod. Phys.*, vol. 94, p. 015004, Feb 2022. [Online]. Available: <https://link.aps.org/doi/10.1103/RevModPhys.94.015004>
- [11] D. A. Fedorov, B. Peng, N. Govind, and Y. Alexeev, “Vqe method: a short survey and recent developments,” *Materials Theory*, vol. 6, no. 1, p. 2, Jan 2022. [Online]. Available: <https://doi.org/10.1186/s41313-021-00032-6>
- [12] W. J. Huggins, J. R. McClean, N. C. Rubin, Z. Jiang, N. Wiebe, K. B. Whaley, and R. Babbush, “Efficient and noise resilient measurements for quantum chemistry on near-term quantum computers,” *npj Quantum Information*, vol. 7, no. 1, p. 23, Feb 2021. [Online]. Available: <https://doi.org/10.1038/s41534-020-00341-7>
- [13] K. Klymko, C. Mejuto-Zaera, S. J. Cotton, F. Wudarski, M. Urbanek, D. Hait, M. Head-Gordon, K. B. Whaley, J. Moussa, N. Wiebe, W. A. de Jong, and N. M. Tubman, “Real-time evolution for ultracompact hamiltonian eigenstates on quantum hardware,” *PRX Quantum*, vol. 3, p. 020323, May 2022. [Online]. Available: <https://link.aps.org/doi/10.1103/PRXQuantum.3.020323>
- [14] H.-Y. Huang, R. Kueng, and J. Preskill, “Predicting many properties of a quantum system from very few measurements,” *Nature Physics*, vol. 16, no. 10, pp. 1050–1057, Oct 2020. [Online]. Available: <https://doi.org/10.1038/s41567-020-0932-7>
- [15] J. Wu and T. H. Hsieh, “Variational thermal quantum simulation via thermofield double states,” *Phys. Rev. Lett.*, vol. 123, p. 220502, Nov 2019. [Online]. Available: <https://link.aps.org/doi/10.1103/PhysRevLett.123.220502>
- [16] D. Zhu, S. Johri, N. M. Linke, K. A. Landsman, C. H. Alderete, N. H. Nguyen, A. Y. Matsuura, T. H. Hsieh, and C. Monroe, “Generation of thermofield double states and critical ground states with a quantum computer,” *Proceedings of the National Academy of Sciences*, vol. 117, no. 41, pp. 25 402–25 406, 2020. [Online]. Available: <https://www.pnas.org/doi/abs/10.1073/pnas.2006337117>
- [17] S. McArdle, T. Jones, S. Endo, Y. Li, S. C. Benjamin, and X. Yuan, “Variational ansatz-based quantum simulation of imaginary time evolution,” *npj Quantum Information*, vol. 5, no. 1, p. 75, Sep 2019. [Online]. Available: <https://doi.org/10.1038/s41534-019-0187-2>
- [18] M. Motta, C. Sun, A. T. K. Tan, M. J. O’Rourke, E. Ye, A. J. Minnich, F. G. S. L. Brandão, and G. K.-L. Chan, “Determining eigenstates and thermal states on a quantum computer using quantum imaginary time evolution,” *Nature Physics*, vol. 16, no. 2, pp. 205–210, Feb 2020. [Online]. Available: <https://doi.org/10.1038/s41567-019-0704-4>
- [19] A. Paetznick and K. M. Svore, “Repeat-until-success: Non-deterministic decomposition of single-qubit unitaries,” *Quantum Info. Comput.*, vol. 14, no. 15–16, p. 1277–1301, nov 2014.
- [20] M. S. Moreira *et al.*, “Realization of a quantum neural network using repeat-until-success circuits in a superconducting quantum processor,” 12 2022.
- [21] A. R. Calderbank, E. M. Rains, P. W. Shor, and N. J. A. Sloane, “Quantum error correction and orthogonal geometry,” *Phys. Rev. Lett.*, vol. 78, pp. 405–408, Jan 1997. [Online]. Available: <https://link.aps.org/doi/10.1103/PhysRevLett.78.405>
- [22] S. Aaronson and D. Gottesman, “Improved simulation of stabilizer circuits,” *Physical Review A*, vol. 70, no. 5, nov 2004. [Online]. Available: <https://doi.org/10.1103/>

[2Fphysreva.70.052328](https://arxiv.org/abs/2009.09063)

- [23] B. G. Bodmann, M. Le, L. Reza, M. Tobin, and M. Tomforde, “Frame theory for binary vector spaces,” 2009, arXiv: 0906.3467.
- [24] D. Gottesman, “Stabilizer codes and quantum error correction,” Ph.D. dissertation, California Institute of Technology, 1997.
- [25] A. T. Schmitz, “Gauge structures: From stabilizer codes to continuum models,” *Annals of Physics*, vol. 410, p. 167927, 2019. [Online]. Available: <http://www.sciencedirect.com/science/article/pii/S0003491619301824>
- [26] M. S. A. et al, “Qiskit: An open-source framework for quantum computing,” 2021.
- [27] Q. Sun, T. C. Berkelbach, N. S. Blunt, G. H. Booth, S. Guo, Z. Li, J. Liu, J. D. McClain, E. R. Sayfutyarova, S. Sharma, S. Wouters, and G. K.-L. Chan, “Pyscf: the python-based simulations of chemistry framework,” *WIREs Computational Molecular Science*, vol. 8, no. 1, Sep. 2017. [Online]. Available: <https://doi.org/10.1002/wcms.1340>
- [28] S. B. Bravyi and A. Y. Kitaev, “Fermionic quantum computation,” *Annals of Physics*, vol. 298, no. 1, pp. 210–226, may 2002. [Online]. Available: <https://doi.org/10.1006%2Faphy.2002.6254>
- [29] P. Jordan and E. Wigner, “Über das paulische Äquivalenzverbot,” *Zeitschrift für Physik*, vol. 47, no. 9-10, pp. 631–651, Sep. 1928. [Online]. Available: <https://doi.org/10.1007/bf01331938>
- [30] P. K. Barkoutsos, J. F. Gonthier, I. Sokolov, N. Moll, G. Salis, A. Fuhrer, M. Ganzhorn, D. J. Egger, M. Troyer, A. Mezzacapo, S. Filipp, and I. Tavernelli, “Quantum algorithms for electronic structure calculations: Particle-hole Hamiltonian and optimized wave-function expansions,” *Physical Review A*, vol. 98, no. 2, aug 2018. [Online]. Available: <https://doi.org/10.1103%2Fphysreva.98.022322>